The 8th European Congress on Computational Methods in Applied Sciences and Engineering
ECCOMAS Congress 2022
5-–9 June 2022, Oslo, Norway

MODELIZATION OF A MOLTEN SALT THERMAL ENERGY STORAGE FOR CONCENTRATED SOLAR POWER.

Jordi Vera[1], Guillem Colomer[1], Oriol Sanmartí[1] and C. D. Perez-Segarra[1]

[1] Heat and Mass Transfer Technological Center, Technical University of Catalonia
Carrer de Colom 11, 08222 Terrassa (Barcelona), Spain; www.cttc.upc.edu
{jordi.vera.fernandez, guillem.colomer, oriol.sanmarti, cdavid.perez.segarra}@upc.edu

Key words: CONCENTRATED SOLAR POWER, THERMAL ENERGY STORAGE, HEAT AND MASS TRANSFER, COMPUTATIONAL FLUID DYNAMICS

Abstract. A numerical model for studying a storage tank for concentrated solar power is presented. The model consists of solving the heat equation for the solid part made from ceramic materials, a one-dimensional model for the molten salt circulating inside the solid, and a coupling between them. Then, some results are presented for a reference case with some typical parameters for the storage system.

1 INTRODUCTION

The need for transitioning toward renewable energies is necessary due to climate change and the current energy models unsustainability. Computational methods are a very powerful tool for the design and optimization of systems, in order to improve their efficiency and reliability and to reduce cost and environmental impact. Concentrated Solar Power (CSP) is a renewable energy source that uses sunlight to heat elements at very high temperatures. Solar towers are an important CSP system that consists of a field with multiple mirrors (heliostats) that point to a single region called the receiver. There, a heat transfer fluid (HTF), usually a molten salt, is heated at high temperatures and stored in a hot tank. The HTF is used, when needed, to generate vapor in a steam generator and to produce electricity through a Rankine cycle. The molten salt is then stored in a cold tank waiting for the opportunity of being heated in the receiver again. This is the conventional two-tank energy storage system [1]. However, to reduce costs, a single tank system is an interesting option: the thermocline system with filler [2, 3]. These accumulators consist of huge structures with filler materials of rocks and sand. Then, when the solar field might not provide energy due to nighttime or adverse climate conditions, the accumulated thermal energy in both the molten salts and the filler material can be used to keep powering the plant.

An interesting concept has emerged using industrial waste ceramic material that can be used in structured thermocline systems that consist of channels where the HTF flows inside them. The main objective of this work is to simulate this type of thermal energy accumulator under different working conditions and cycles, using advanced numerical methods to solve the heat equation in the solid domain, and couple it with the molten salt flow in the channels using unsteady 1D models. The flow in these applications is usually laminar, and then very dependent

on the geometry and boundary conditions. Therefore, the possibility of numerically solving the fluid flow in detail using the Navier-Stokes equations will be assessed.

2 GEOMETRY AND OPERATION PARAMETERS

2.1 GEOMETRY

The objective is to simulate the heat storage system. Figure 1 shows the geometry of the solid that will be evaluated. The domain consists of a solid part (bed) with holes inside it that can transport molten salts. Figure 2 shows a cross-section of the solid with different possibilities of hole arrangement. The molten salt is stored in the channels of the solid, and also at the bottom and top of the tank. The bottom of the tank has a fixed quantity of molten salt, but the top of the tank allows a free range of movement to compensate for the density differences of the molten salt due to its temperature dependence.

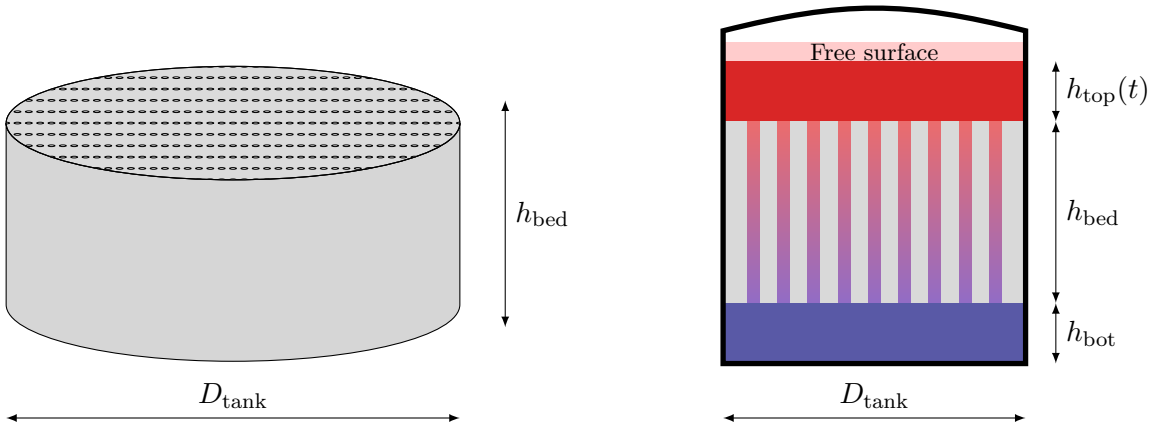

(a) Solid geometry (b) Molten salt channels section

Figure 1: Schematics and geometrical parameters of the storage tank

The diameter of the tank is in the order of $D_{\text{tank}} \approx 45$ m, the height is in the order of 14 m. The holes inside the channel are approximately 10 mm, with a separation between them of 20 mm. In this configuration, the number of holes on the tank is approximately 3 000 000 holes.

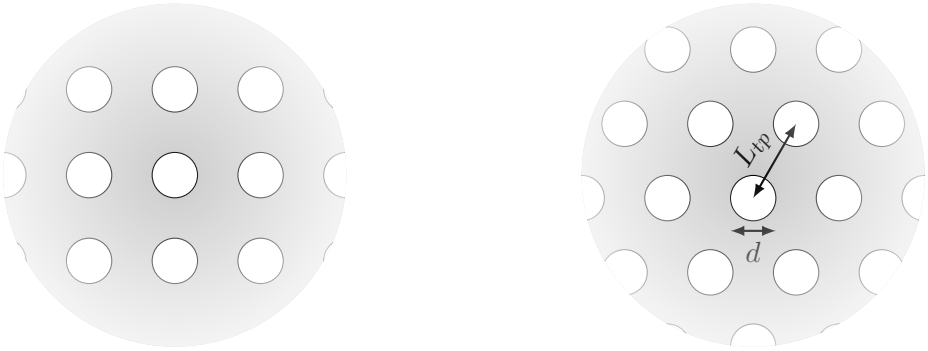

(a) 90 degree arrangement case

(b) 30 degree arrangement case

Figure 2: Cross section of the bed. The solid is represented in gray and the channels in white.

2.2 OPERATIONAL PARAMETERS

The operation regime of the thermal storage system has 3 operation modes; Charging, discharging and idle. When the energy received from the solar field is greater than the one consumed by the power block, the remaining energy is stored using the charge cycle. This cycle consists of molten salt circulating at a high temperature from the top of the tank to the bottom of the tank, see Figure 3a. The thermal energy is stored in the solid, and also in the accumulated molten salt at the top, channels, and bottom of the system. The system keeps getting charged until the temperature at the bottom reaches a certain threshold called the cutoff temperature. Then the system remains at wait during some idle time depending on the plant operation.

When the energy received from the solar field is not enough for the power block, the discharging cycle is started. This cycle consists of the molten salt circulating at a low temperature from the bottom of the tank to the top of the tank, see Figure 3b. The previously stored thermal energy is transferred back to the molten salt and used to supply energy to the power block. The system is in discharge mode until the molten salt discharge temperature drops below a certain threshold (another cutoff temperature). Then, the system remains idle for some time and all the process is repeated. Other operational modes of the plant can also be established.

(a) Charge cycle

(b) Discharge cycle

Figure 3: Charge and discharge cycles

In the case of this study, the cycle shown in Figure 4 is considered. Despite not being a physically realistic cycle for CSP (no sun hours are considered), it allows us to define a reference case and study different tank configurations. The cycle follows the same principle as explained before, however, the idle time for the charging and discharging cycles is set to zero.

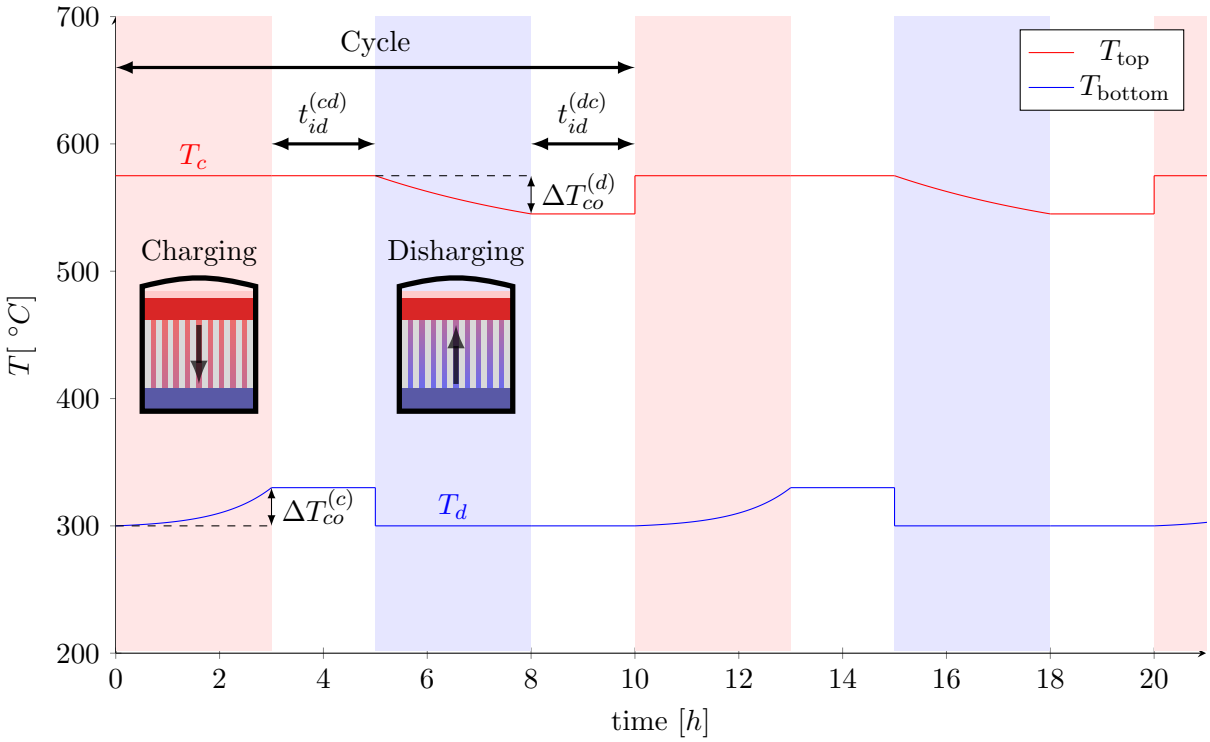

Figure 4: Example of a set of operating cycles

3 NUMERICAL SET-UP

3.1 Studied domain

To evaluate the case, the solid domain is simulated by solving the three-dimensional heat equation. The fluid domain is solved considering a one-dimensional simplified version of the Navier-Stokes equations (more detail on Section 3.3). The solid and fluid domains are coupled at the interface considering a Conjugate Heat Transfer (CHT) approach.

Given the magnitude of the case, it is obvious that discretizing all the domains to solve the heat equation is not feasible. A rough estimation is that even using a coarse mesh the needed mesh elements would be 60 000 Million cells. To be able to simulate the case, some simplifications and assumptions are made. If the effects of the heat loss at the lateral walls are neglected, a periodic domain can be considered. An adiabatic boundary condition for the periodic walls can then be considered. Figure 5a shows two possible domains that can be studied for the staggered hole arrangement (even a smaller region could be defined with periodic boundary conditions).

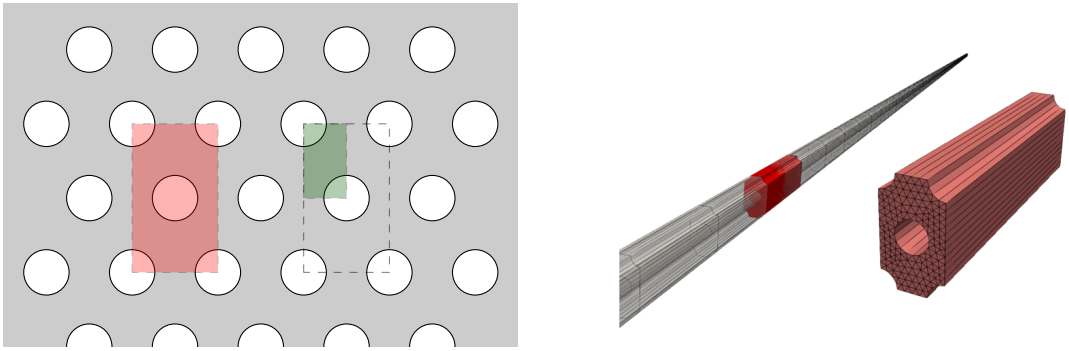

(a) Possible periodic domains

(b) Solid meshing (extrusion, and single element)

Figure 5: Domain and discretization of the solid for the 30 degree arrangement case

3.2 Mesh

The solid section is discretized with two-dimensional elements and then the mesh is extruded at the z direction with a given number of planes of extrusion. Figure 5b shows an illustrative example of this meshing, although the mesh used for the results is finer and considers the smaller domain shown in Figure 5a.

For the fluid, a one-dimensional mesh is used. An illustrative example of each mesh cell is shown in Figure 6. The fluid mesh is coincident at the interface of the solid mesh, i.e. the extrusion dimension Δz is the same for the fluid and the solid, and all the height of the tank is considered in this domain.

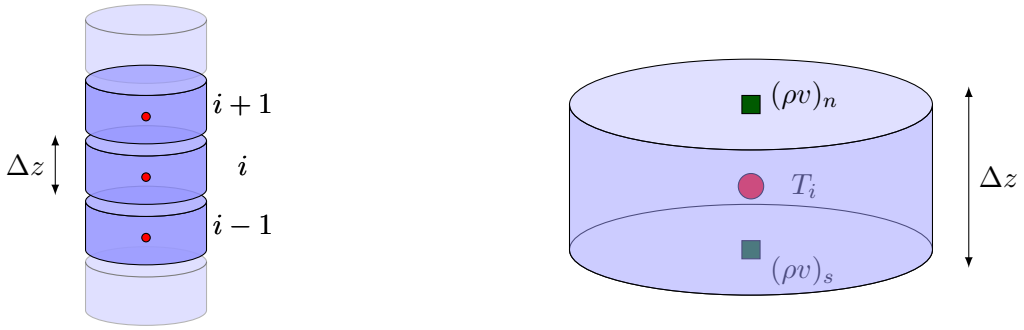

Figure 6: Fluid discretization

Apart from the discretization of the channels of the fluid, two large control volumes are considered at the top and bottom domains of the tank. The top control volume has the particularity that can change its height depending on the density variations due to temperature variations.

3.3 Equations

For the solid, the classical heat equation is numerically solved. Some thermal properties have dependence on the temperature. Then the approach used when solving the discrete heat

equation has to consider this dependence. The continuous form of the heat equation is shown as follows:

$$\rho c_p \frac{\partial T}{\partial t} = \nabla \cdot (\lambda \nabla T) \tag{1}$$

where ρ, c_p, λ are the density, specific heat, and thermal conductivity respectively. For the walls in contact with the fluid, a convective boundary condition is considered, where the convection coefficient and fluid temperature is evaluated at each section based on a prescribed value of the Nusselt number (usually laminar flow). The rest of the walls are set to adiabatic boundary conditions. The equations are discretized in time using an implicit approach.

For the fluid, the continuity, momentum and energy equations are considered for a 1D unsteady case. The continuity equation will give the velocity magnitude, that is not constant due to the temperature dependence of the molten salt density.

$$\frac{\rho_i - \rho_i^0}{\Delta t} \Delta z = (\rho v)_s - (\rho v)_n \tag{2}$$

where v is the velocity on the z direction, that can be positive (discharging cycle) or negative (charging cycle). The sub-index $_i$ refers to the fluid nodal index (see Figure 6) in a staggered arrangement. The sub-indexes $_s$ and $_n$ correspond to the properties evaluated at the bottom and top faces of the cell respectively. The super-index ^{0} indicates the value at the previous time iteration, while the values without super-index indicate the current time instant. The energy equation will give the temperature at each main node value (see Figure 6). The discrete form is shown:

$$\begin{aligned} \rho_i^0 \overline{c_{p_i}} \frac{T_i - T_i^0}{\Delta t} =& \frac{1}{\Delta z} \left((\rho v)_s \overline{c_{p_s}} (T_s - T_i) - (\rho v)_n \overline{c_{p_n}} (T_n - T_i) \right) \\ &+ \frac{\lambda_s}{\Delta z^2} (T_{i-1} - T_i) + \frac{\lambda_n}{\Delta z^2} (T_{i+1} - T_i) + \dot{q}_{\mathcal{V}} \end{aligned} \tag{3}$$

The thermophysical properties are dependent on temperature. Then they are evaluated accordingly, depending on the type of molten salt used (see [4]). In our case the Solar Salt is used. The term $\rho_i^0 \overline{c_{p_i}}$ of the left-hand-side is evaluated at the mean temperature. The term $\dot{q}_{\mathcal{V}}$ is a heat source term that is determined when imposing the coupling between the solid and the fluid domains.

The momentum equation gives the pressure loss, which in discrete form is:

$$\frac{\rho_i v_i - \rho_i^0 v_i^0}{\Delta t} = \frac{1}{\Delta z} \left((\rho v^2)_s - (\rho v^2)_n \right) + \frac{1}{\Delta z} (P_s - P_n) - f_i \frac{\rho_i v_i |v_i|}{2} \frac{\Delta S_{\text{lat}}}{\Delta \mathcal{V}_i} - \rho_i g \tag{4}$$

where P is the pressure, f the friction factor, ΔS_{lat} is the lateral surface of the control volume, and $\Delta \mathcal{V}_i$ is the volume of the control volume. However, in the evaluated cases the effect of all terms, except the gravitational forces were shown to be all negligible.

For the top and bottom buffer regions, global balances of mass and energy are applied.

3.4 General algorithm

Here the algorithm is summarized. A semi-implicit approach is used to do the coupling between the solid and the fluid.

Input physical parameters, geometrical parameters, and initial conditions (T_{solid}, T_{fluid})
Input numerical parameters
Preprocess to define fluid control volume and relate the neighbour solid cells
Initial conditions : Start fluid at T_f^0
Initial conditions : Start solid at T_s^0
$t = 0$
while $t < t_{end}$ **do**
    Calculate physical properties of the fluid (at t^n or extrapolating)
        Calculate velocity from continuity equation
        Calculate local convection heat coefficient α_i^n
    Calculate $\dot{Q}^n_{\text{conv},i}$ for each fluid control volume i
    Calculate the new fluid temperatures ($t_f^n \rightarrow t_f^{n+1}$)
        Modify matrix/vector coefficients of fluid equations
        Solve the system (e.g. TDMA)
    Calculate physical properties of the solid (at t^n or extrapolating)
    Calculate the new solid temperatures ($t_s^n \rightarrow t_s^{n+1}$)
        Modify matrix $\vec{A}$ and vector $\vec{b}$ coefficients of solid equations ($\vec{A}\vec{T}_{\text{solid}} = \vec{b}$)
            Update physical properties at the cells
            Update convective boundary conditions at each solid-fluid boundary
        Solve the system $\vec{A}\vec{T}_{\text{solid}} = \vec{b}$
    Calculate pressure loss
    Update $t = t + \Delta t$
end while
Print results and post-processing

4 RESULTS

4.1 Reference case

A reference case with fixed geometrical and operational parameters is computed. Here some results are presented to show the capabilities of the model. The solid solver gives the transient solution of the temperature distribution in three dimensions. Figure 7 shows a color map distribution of temperatures of a section of the solid for a given time instant.

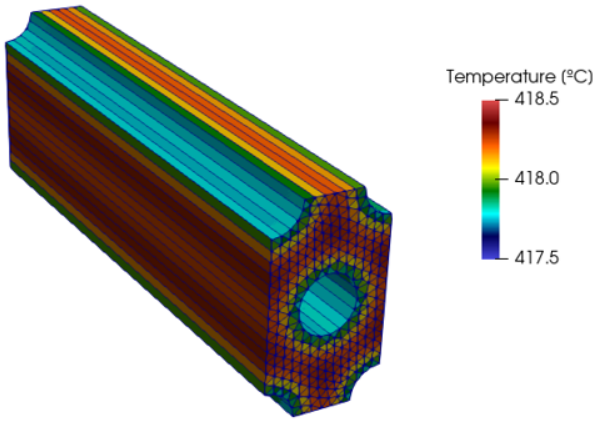

Figure 7: Temperature distribution of a solid section

Another output that the code can provide is the temperature of the molten salt at the different heights of the tank. Figure 8 shows the molten salt temperature over the height of the tank for different time instants, corresponding to a charge-discharge cycle, once the simulation has reached a statistically stationary state. It can be observed that the molten salt temperature ends up having a somewhat linear profile.

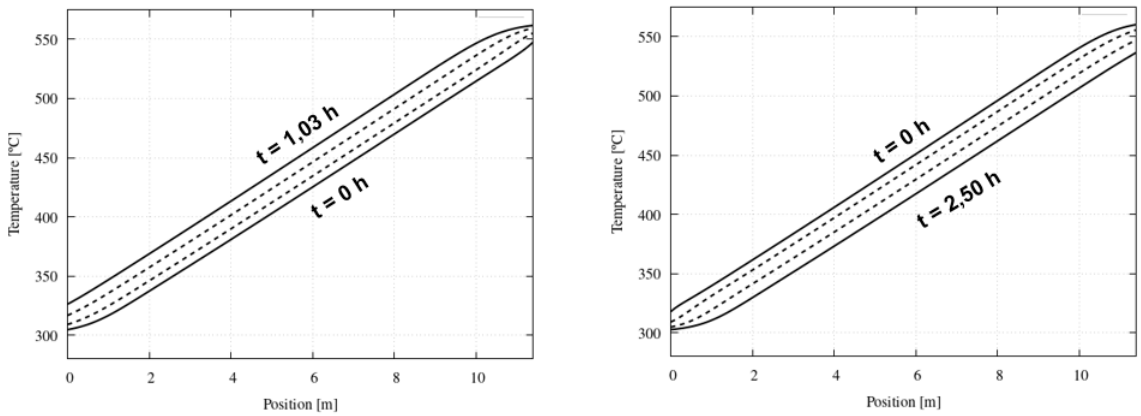

(a) Charge cycle

(b) Discharge cycle

Figure 8: Temperature of the molten salt as a function of height and time.

The top and bottom mean temperatures in the buffer regions are used to control the charge and discharge cycles with the cutoff temperature parameter. The duration of the cycles, and therefore the accumulated energy, is very dependent on this temperature and where it is evaluated. Figure 9 shows the evolution of temperature over time for different regions for the top and bottom. These positions are the top/bottom layer of the solid, molten salt at the edge of the bed and molten salt at the center, and top/bottom of the buffer zone. It can be observed that there is a small delay between the fluid temperature (red line) and the solid temperature (black

line). This delay gives an insight of the heat transfer efficiency between the fluid and the solid. It can also be observed that the buffer regions (blue lines) add an additional thermal inertia to the temperature making the cycles last longer.

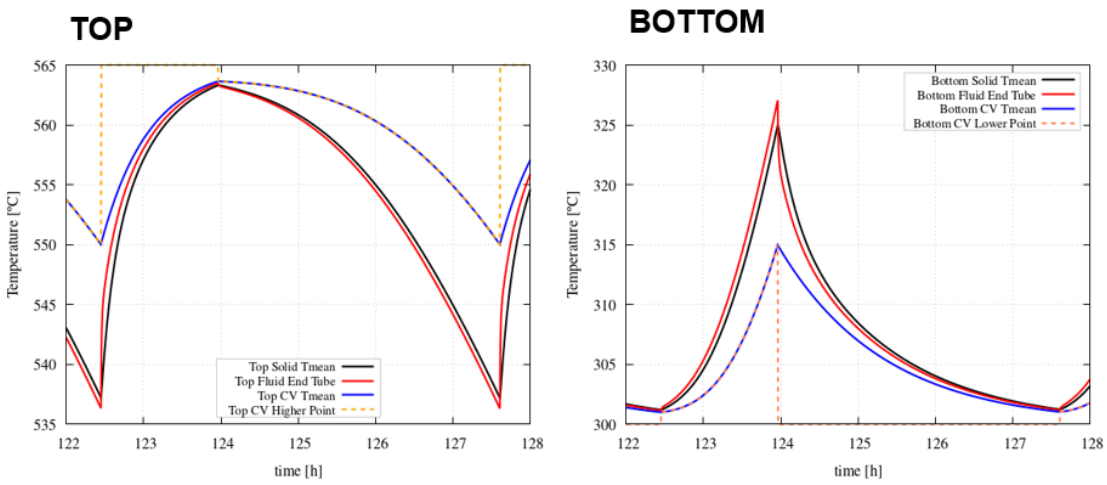

Figure 9: Temperature evolution over time for the top and bottom

4.2 Nusselt number

To calculate the heat transfer between the solid and the fluid, a convection boundary condition is used. This boundary condition has the following issue: The Nusselt number Nu used to calculate this coefficient, (in the case of laminar flows like the one studied) have a strong dependence on the boundary conditions. For instance, if a constant temperature is considered at the walls, the Nu number takes a value of $Nu = 3.66$, while if a constant heat flow is considered, $Nu = 4.36$. In the studied case, the temperature profile at the wall is more similar to a linear one (as seen in Figure 8). To estimate a proper Nusselt number, an independent case is tested.

The case consists of solving the Navier-Stokes equations for a tube with adequate boundary conditions at the walls, in this case, a linear temperature profile. This case is independent and does not consider coupling with the solid for now. The next step (not included in this paper) will be to couple both simulations.

First, a test is done numerically solving the Navier-Stokes equations and calculating the Nusselt number for the boundary conditions of constant temperature and constant heat flow. These results are used as a validation and match with the already known solution of $Nu = 3.66$ for constant wall temperature and $Nu = 4.36$ for constant heat flux. Knowing that the model works well, the new specific boundary condition is applied and the Nusselt number obtained is used on the model. In this case, the value of the Nusselt is a bit higher than the 4.36 of the constant heat flux.

5 CONCLUSIONS

A numerical model for studying a thermal storage tank is presented. The model is capable of giving the three-dimensional transient temperature distribution of the solid, a one-dimensional

transient profile of the molten salt temperature, and the overall accumulated energy on the tank for each cycle. The presented model can be used for studying and optimizing the heat accumulator configuration. Several geometrical and operational parameters can be modified to find a more suitable configuration. Given the relatively low computational cost of the model, several independent cases can be run in parallel to optimize the storage tank.

Moreover, the model is the first step to extending the methodology to consider a Conjugate Heat Transfer (CHT) problem solving the multidimensional Navier-Stokes equations for the molten salt and the heat equation of the solid. The calculation of the heat transfer can be improved if the solid heat equation and the fluid Navier-Stokes equations are coupled with a CHT approach. The challenges of this approach are the communication between the two cases and their parallelization. The faces of the boundaries between interfaces should be conformed and belong to the same core to ease the communication. Additionally, there would be a need to increase the computing power given the computational demand of the Navier-Stokes equations, also considering that the different time scales of the fluid and solid solutions might add the need of using different timesteps for the fluid and solid parts.

ACKNOWLEDGEMENTS

This work has been carried out in the framework of the Newcline project, which is supported under the umbrella of CSP-ERA.NET 1st Cofund Joint Call, and by the following National Agencies: AEI (Spain), CDTI (Spain), Jülich (Germany), SFOE (Switzerland). CSP-ERA.NET is supported by the European Commission within the EU Framework Programme for Research and Innovation HORIZON 2020 (Cofund ERA-NET Action, N° 838311).
J. Vera has been financially supported by the Ministerio de Educación y Ciencia (MEC), Spain, (FPI grant PRE2018-084017).

REFERENCES

[1] Ugo Pelay, Lingai Luo, Yilin Fan, Driss Stitou, and Mark Rood. Thermal energy storage systems for concentrated solar power plants. *Renewable and Sustainable Energy Reviews*, 79:82–100, 2017.

[2] PA Galione, Carlos David Pérez-Segarra, I Rodríguez, A Oliva, and J Rigola. Multi-layered solid-pcm thermocline thermal storage concept for csp plants. numerical analysis and perspectives. *Applied energy*, 142:337–351, 2015.

[3] Ignacio González, Carlos David Pérez-Segarra, Oriol Lehmkuhl, Santiago Torras, and Assensi Oliva. Thermo-mechanical parametric analysis of packed-bed thermocline energy storage tanks. *Applied energy*, 179:1106–1122, 2016.

[4] Alexander Bonk, Salvatore Sau, Nerea Uranga, Marta Hernaiz, and Thomas Bauer. Advanced heat transfer fluids for direct molten salt line-focusing CSP plants. *Progress in Energy and Combustion Science*, 67:69–87, 2018.